

Titre: Comparison of antimicrobial properties of inorganic peroxide
Title: polymer composites

Auteurs: Dario Job, Joane Matta, Cat-Thy Dang, Yara Raphael, Joshua
Authors: Vorstenbosch, Bentolhoda Helli, Géraldine Merle, & Jake E. Barralet

Date: 2024

Type: Article de revue / Article

Référence: Job, D., Matta, J., Dang, C.-T., Raphael, Y., Vorstenbosch, J., Helli, B., Merle, G., &
Citation: Barralet, J. E. (2024). Comparison of antimicrobial properties of inorganic peroxide
polymer composites. MedComm – Biomaterials and Applications, 3(1), e75 (13
pages). <https://doi.org/10.1002/mba2.75>

Document en libre accès dans PolyPublie

Open Access document in PolyPublie

URL de PolyPublie: <https://publications.polymtl.ca/57908/>
PolyPublie URL:

Version: Version officielle de l'éditeur / Published version
Révisé par les pairs / Refereed

Conditions d'utilisation: Creative Commons Attribution 4.0 International (CC BY)
Terms of Use:

Document publié chez l'éditeur officiel

Document issued by the official publisher

Titre de la revue: MedComm – Biomaterials and Applications (vol. 3, no. 1)
Journal Title:


Maison d'édition: John Wiley & Sons
Publisher:

URL officiel: <https://doi.org/10.1002/mba2.75>
Official URL:

Mention légale: This is an open access article under the terms of the Creative Commons Attribution
Legal notice: License (<https://creativecommons.org/licenses/by/4.0/>), which permits use, distribution
and reproduction in any medium, provided the original work is properly cited

ORIGINAL ARTICLE

Comparison of antimicrobial properties of inorganic peroxide polymer composites

Dario Job¹ | Justin Matta² | Cat-Thy Dang¹ | Yara Raphael¹ |
Joshua Vorstenbosch² | Bentolhoda Helli¹ | Geraldine Merle^{1,2}  |
Jake Barralet^{2,3}

¹Chemical Engineering Department,
Polytechnique, Montreal, Québec,
Canada

²Department of Surgery, Division of
Surgical and Interventional Sciences,
McGill University, Montreal, Québec,
Canada

³Faculty of Dentistry, McGill University,
Montreal, Québec, Canada

Correspondence

Geraldine Merle, Chemical Engineering
Department, Polytechnique, Montreal,
QC, Canada.

Email: geraldine.merle@polymtl.ca

Funding information

Natural Sciences and Engineering
Research Council of Canada; Fonds de
Recherche du Québec - Santé

Abstract

Wound healing and prevention of bacterial infections are critical aspects of modern medical care. In this work, antibacterial films were produced by creating composites of polycaprolactone with inorganic peroxides. Calcium, magnesium, and zinc peroxide were incorporated in a biocompatible polymeric film. Iron oxide, sodium bicarbonate, and calcium phosphate were added to reduce hydrogen peroxide and to maintain pH in a less alkaline range, allowing for optimization of the material's antibacterial efficacy while minimizing cytotoxicity toward human fibroblasts. Experiments with common wound pathogens, *Staphylococcus aureus* and *Pseudomonas aeruginosa*, confirmed significant and prolonged antibacterial effects of peroxide-doped films. Findings showed that the addition of CaO₂ and MgO₂ within the film increased cytotoxicity toward human fibroblasts after 48 h (30%–40% decrease compared to control), whereas ZnO₂-based films exhibited a minimal cytotoxicity consistently maintaining over 70% cell viability throughout the course of the experiment. We examined the materials' sustained release of reactive oxygen species and oxygen, and pH variation correlated with antibacterial activity. Given the unique combination of antibacterial efficacy and mammalian biocompatibility, these peroxides have value as components to sustain hydrogen peroxide release when appropriately compounded to reduce pH variation and avoid excessive hydrogen peroxide levels.

KEYWORDS

bacteria, hydrogen peroxide, inorganic, oxygen, peroxide, wound

Dario Job, Justin Matta, Geraldine Merle, and Jake Barralet contributed equally.

This is an open access article under the terms of the [Creative Commons Attribution](https://creativecommons.org/licenses/by/4.0/) License, which permits use, distribution and reproduction in any medium, provided the original work is properly cited.

© 2024 The Authors. *MedComm – Biomaterials and Applications* published by John Wiley & Sons Australia, Ltd on behalf of Sichuan International Medical Exchange & Promotion Association (SCIMEA).

1 | INTRODUCTION

Since the discovery of penicillin a century ago, antibiotics are now routinely used to treat bacterial infections.¹ There are several antibiotics classified into penicillins, cephalosporins, aminoglycosides, tetracyclines, macrolides, and fluoroquinolones that can be used depending on the type and severity of the infection. However, concurrent with antibiotic clinical use, the emergence of antimicrobial resistance (AMR) has become a significant and pressing concern. The widespread use and over-reliance on antibiotics have facilitated the natural selection of resistant strains among microbial populations. Indeed, over the years, bacteria causing common or severe infections such as *Staphylococcus aureus*, *Escherichia coli*, *Enterococcus faecium*, *Streptococcus pneumoniae*, and *Pseudomonas aeruginosa* have undergone adaptive changes that have conferred resistance to antibiotics. In 2019, ~5 million deaths globally were attributable to AMR.² The escalating prevalence of AMR can be ascribed, in part, to the unmonitored or incorrect use of antibiotics.³ In an attempt to mitigate this increasingly sophisticated antibiotic and antibiotic-loaded dressings are being developed.³

As alternatives to antibiotics, new strategies such as antimicrobial peptides (AMPs) that disrupt lipid bilayer structures are being developed.^{4–6} However, resistance to AMPs has also emerged.^{7,8} Improvements in first-generation bactericidal materials that chemically destroy bacteria have subsequently attracted renewed interest, especially if they can be applied topically or as implantable coatings. For example, as the development of photography facilitated the study of colloidal silver, now often referred to as nano silver, there were several reports of its use in the treatment of erysipelas, strep, gonorrhea, and typhoid between 1900 and 1930s. This approach was largely abandoned when the effectiveness of antibiotics became apparent, such that between 1930 and 1980 there were very few reports of nano- or colloidal silver to treat bacterial infections. But in the past 23 years alone, there have been more than 10,000 publications. In addition to silver nanoparticles, weak antiseptics such as potassium permanganate have been used. More effective compounds such as carbolic acid, mercuric chloride, and hydrogen peroxide are of limited value due to their corrosive or toxic properties. Sodium hypochlorite and boric acid in a neutralizing solution provided an effective but chemically unstable direct contact antiseptic for wounds. To overcome this instability, a slow drip continuous flush known as the Carrel–Dakin process was developed⁹ and is still in use today as the problem of resistance to more specific agents grows.^{10,11} While superficially it may seem counterintuitive to use bleach to disinfect wounds without

damaging tissue, the concentration is low, and the sustained delivery is the key element to disinfection. There are several recent papers confirming that healing even in quite compromised patients occurs without issue.¹²

Due to the low solubility of zinc oxide and zinc hydroxide, zinc peroxide is one of the least caustic solid peroxides. It decomposes slowly in aqueous conditions liberating oxygen and hydrogen peroxide and was used extensively during World War II in the care of wounds or other lesions caused, or secondarily infected, by anaerobic Streptococci, tetanus and anaerobes of the gas gangrene group, *Bacteroides melaninogenicum*, *Bacillus fusiformis*, Actinomyces, and certain Spirochaetes. However, its effectiveness was limited by loss of activation, it needs to be heated before use (presumably to break down any carbonates formed on exposure to air) and reapplied daily, and it sticks to the wound causing a foreign body reaction. To overcome these problems, Reid and Altemeier¹⁰ developed a less adhesive formulation with delayed release of oxygen. Shortly after the widespread clinical application of antibiotics, a 1952 review article claimed that zinc peroxide was superior to sulfonamides and antibiotics in the treatment of gastric ulcers; synergistic gangrene, and only after excision; decubitus ulcers; other ulcers with high rates of infection; diabetic gangrene and ulcerative stomatitis.¹³ Afterwards, the work shifted to other compounds such as benzoyl peroxide.¹⁴

As the threat of AMR increases, solid peroxides are being reconsidered as alternative sources to provide sustained delivery of hydrogen peroxide (H₂O₂). For example, copper peroxide has been evaluated for wound healing or chemokinetic therapy.^{15,16} Metal peroxides can also release oxygen (O₂) and can maintain elevated oxygen levels for several days.^{17–21} Controlling the decomposition products of metal peroxides and reducing the rate of oxygen evolution has been the goal of some previous studies, such as nanoscale metal peroxides.^{16,18,22} Another approach is to encapsulate them in polymers that provide cells or tissues with oxygen for longer periods of time and add catalysts to limit H₂O₂ production.^{23–26}

Here we provide for the first-time comparative data of a selection of three metal peroxides in a polycaprolactone (PCL) film system following the previous identification of parameters affecting hydrogen peroxide or oxygen release²⁷ and the development of a low toxicity formulation with a catalyst to reduce excess hydrogen peroxide formation and a buffer to prevent excessive pH elevation. Calcium peroxide (CaO₂), magnesium peroxide (MgO₂), and zinc peroxide (ZnO₂) were selected due to the history of clinical use of zinc peroxide, the extensive literature on

calcium peroxide for oxygen delivery, and the relative lack of data comparing with magnesium peroxide despite the low toxicity of magnesium ions. They were formulated into films and evaluated for their antimicrobial activity against *S. aureus* and *P. aeruginosa*. They are two of the most common bacteria in a variety of microbial infections and they may respond differently to metal peroxides. Since each metal peroxide has different release properties, kinetic measurements of oxygen, H_2O_2 and reactive oxygen species (ROS) release, and pH variation were conducted and associated with their antibacterial and cytotoxic effects.

2 | RESULTS

2.1 | Physicochemical and mechanical characterization of the composite films

We assembled composite films using zinc-, calcium-, and magnesium peroxides and by combining other components to minimize the cytotoxicity of the samples

attributed to H_2O_2 and pH. Scanning electron micrographs (Figure 1) showed the microstructure of the surface of the samples.

No visible differences were found between morphology of the composite film containing different peroxides. All the samples exhibit a smooth surface with some irregularities indicating that powdered components were not appreciably aggregated at the microscale. The thermal behavior of the samples was studied using thermogravimetric analysis to confirm the composition of the composite (Figure 2A). A two-step degradation process for each material was observed and attributed to the loss of water and decomposition of sodium bicarbonate ($NaHCO_3$) and monocalcium phosphate ($Ca(H_2PO_4)_2$) which take place at $130^\circ C$ and represent a total mass percentage of about 6–6.9 according to Table 2.²⁸ Around $300^\circ C$, the first major weight loss occurred for each sample at the same time as the control, and may be caused by the initial degradation of PCL, which accounts for most of the mass (the control losing more mass as it contains more PCL). In ZP, a slight shoulder appeared around

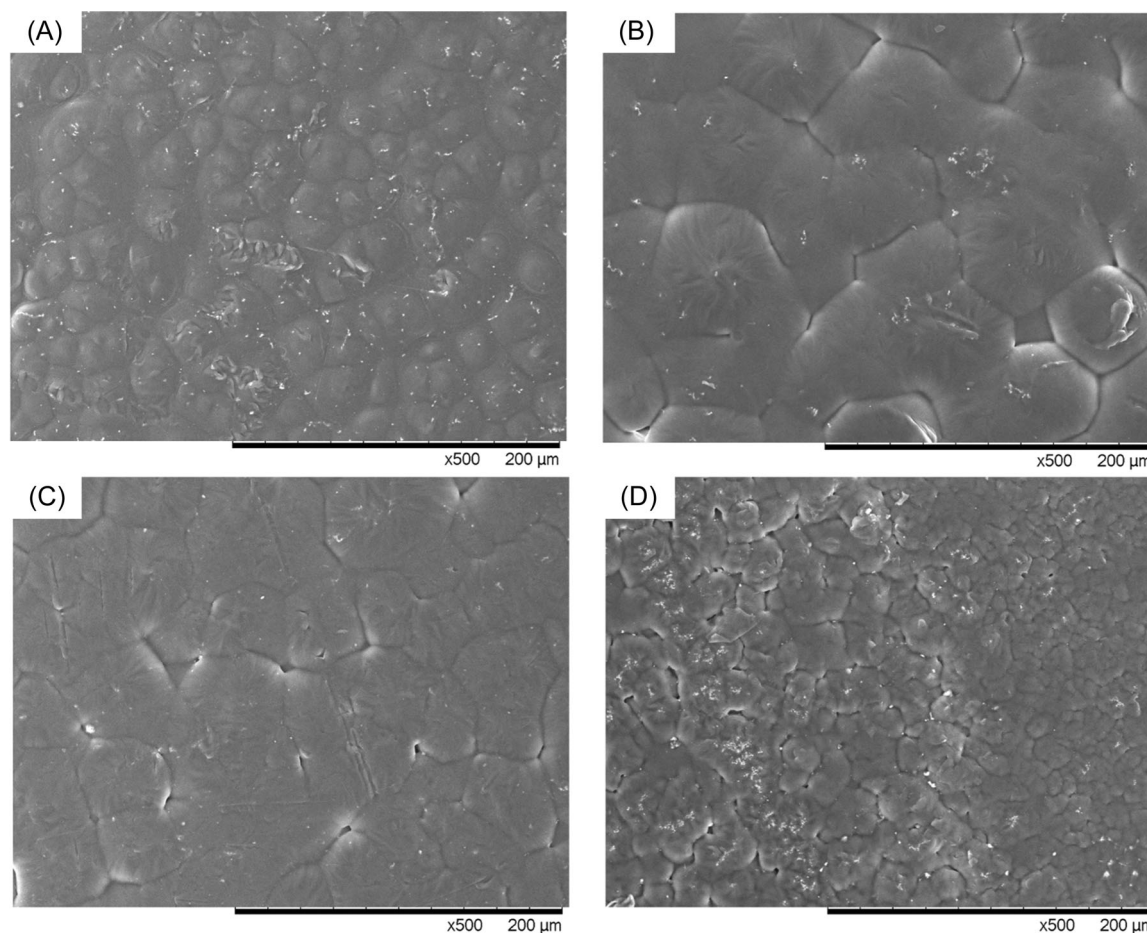


FIGURE 1 Scanning electron micrographs captured at a $\times 500$ magnification illustrating the microstructure of the control and experimental films: (A) control, (B) calcium peroxide, (C) magnesium peroxide, and (D) zinc peroxide.

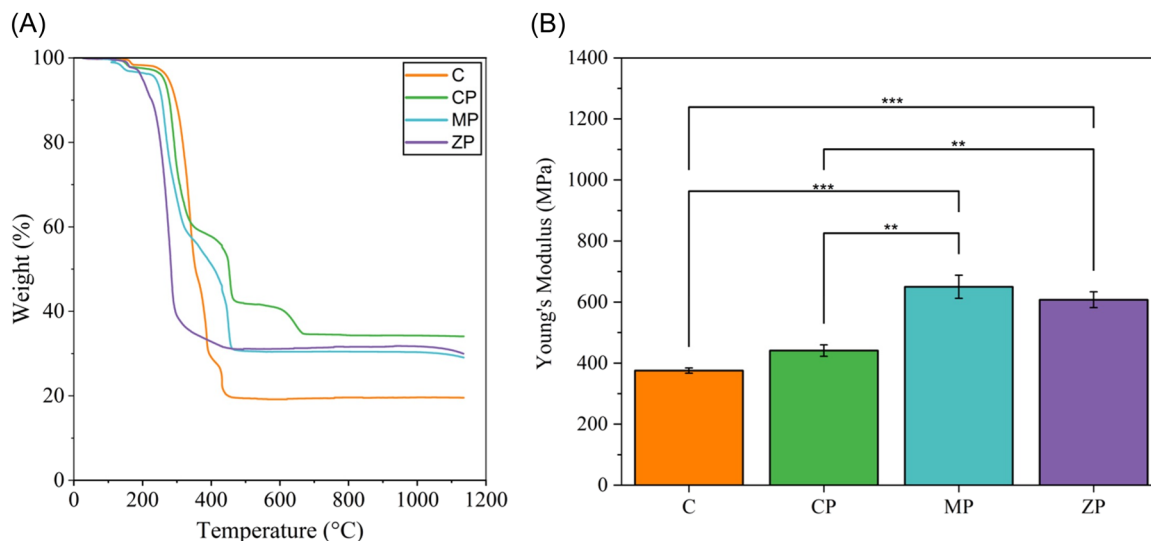


FIGURE 2 (A) Thermogravimetric analysis. (B) Elastic moduli derived from tensile testing (mean \pm SD; $n = 3$). Values indicated by asterisks (*) are statistically different (** $p < 0.01$; *** $p < 0.001$).

210°C corresponding to the degradation of ZnO₂. For MP, a small shoulder appeared during the degradation of PCL around 350°C, which corresponds well to the degradation of magnesium peroxide.²⁹ For CP, CaO₂ decomposed around 450°C into oxygen, H₂O₂, and calcium oxide. This calcium oxide then decomposes at around 600°C, which likely gave rise to the shoulder for CP at this temperature.

All composites had significantly higher Young's modulus compared to control PCL film. The lowest values of modulus of elasticity were recorded at 400 MPa for the peroxide-free control. The highest value of modulus of elasticity was recorded when magnesium and zinc peroxides were incorporated (~600 MPa, Figure 2B). The swelling index of the control film was very small (~1%), and this increased to ~2% for CP and between 3.5% and 5.5% for ZP and MP, indicating higher permeability in these samples (Figure S1).

2.2 | Product degradation release

The oxygen release from the different films was investigated (Figure 3A). No oxygen release was measured in media with control film. For each sample, the greater oxygen release occurred during the first hour and continued to rise gradually until the first and second days. CP produced by far the largest oxygen release ~3 times more than the other peroxides with peak concentrations up to about 90 $\mu\text{M mol}^{-1}$ whereas MP and ZP reached maxima: values of ~20 and 40 $\mu\text{M mol}^{-1}$ respectively.

The antibacterial properties of metal peroxides are thought to be at least partially due to their release of ROS and more particularly H₂O₂.³⁰ The amount of ROS of the initial control values was used as a baseline. The variation in ROS concentration for MP was not statistically significant ($p < 0.05$). For CP and ZP, there was a very slight upward trend and a significant ($p < 0.05$) increase after 1 day in vitro (Figure 3B). However, H₂O₂ concentration (Figure 3C) differed considerably. For CP and MP, the concentration of H₂O₂ gradually increased during the first few hours and then fell at Days 1 and 2, whereas for ZP, the concentration increased throughout the experiment. The maximum reached for MP and ZP were about 50 $\mu\text{M mol}^{-1}$, respectively, at 4 h and 2 days, while CP had higher concentrations up to about twice as much (100 $\mu\text{M mol}^{-1}$). Table 1 shows H₂O₂ release measurements carried out after 18 months' storage of the samples expressed as the percentage of freshly prepared films (cf Figure 3C) CP conserved around 60%, while MP and ZP retained over 90% of their initial release values.

Finally, the pH of the solutions in which the samples were deposited to evaluate their release was also measured since the pH plays an important role in the healing of wounds and especially in the antibacterial effects. The results in Figure 3D show that ZP had little effect on pH. For CP and MP, however, the pH changed dramatically after 24 and 48 h. CP reaches values of about 9.5 and 10 on Days 1 and 2, while MP has values of about 8.3 and 8.8 at the same time points.

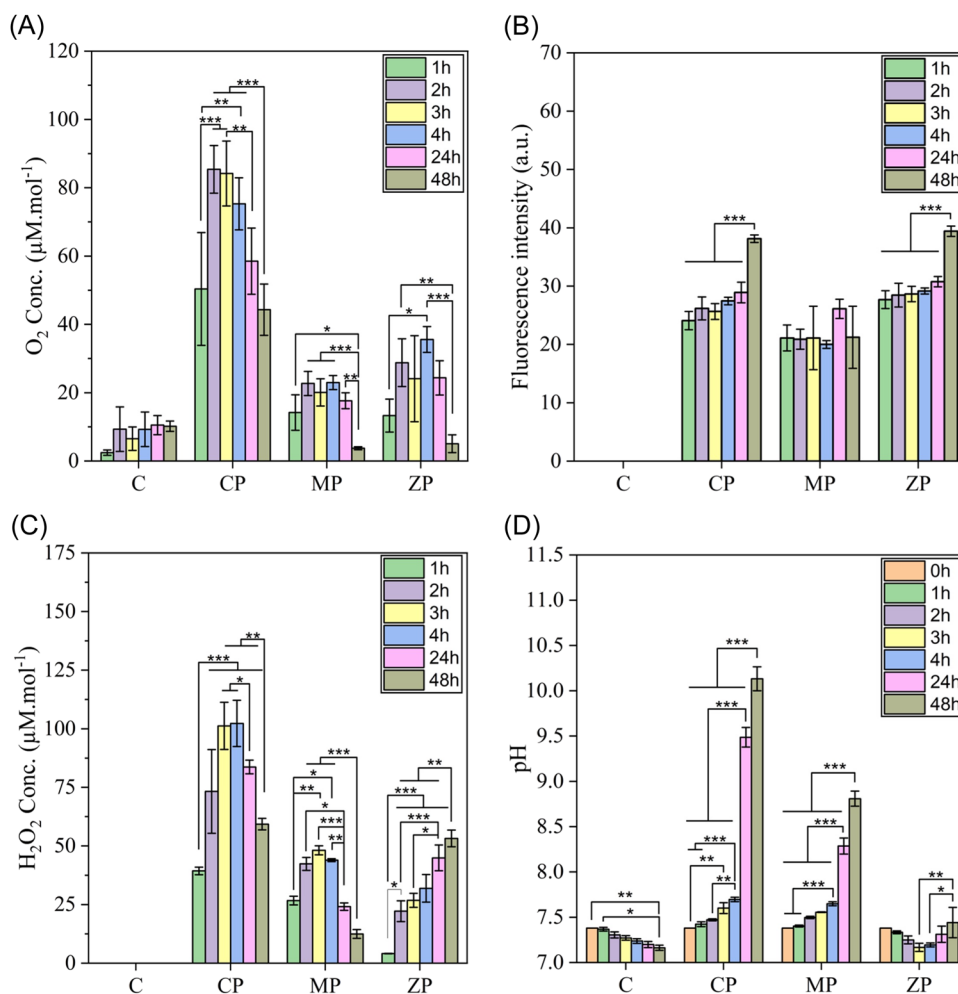


FIGURE 3 (A) O₂ concentration measurements up to 4 h (mean ± SD; $n = 3$). (B) Reactive oxygen species concentration measured as fluorescent intensity with H2DCFDA reagent (mean ± SD; $n = 3$). (C) Hydrogen peroxide release and (D) pH of solutions containing samples measured up to 48 h (mean ± SD; $n = 3$). Values indicated by asterisks (*) are statistically different (* $p < 0.05$; ** $p < 0.01$; *** $p < 0.001$).

TABLE 1 H₂O₂ release from films after 24 and 48 h aqueous immersion after 18 months' storage in ambient laboratory conditions expressed as a percentage of values from freshly prepared films (% mean ± SD).

	24 h	48 h
CP	61.32 ± 3.74	58.81 ± 3.39
MP	89.65 ± 7.45	92.61 ± 13.90
ZP	93.16 ± 16.10	92.43 ± 6.31

2.3 | Bacterial activity and cytotoxicity

The antimicrobial efficacy of the peroxide films against bacteria in solution is shown in Figure 4A,B for *S. aureus*, a Gram-positive bacteria, and *P. aeruginosa*, a Gram-negative bacteria, respectively. The results show that the peroxide-doped samples have a significant and prolonged

effect over the 3 days of the study against both strains of bacteria. CP had the strongest effects on the first day and by the second day no bacteria were detectable. MP had a similar effect but was less effective especially for *S. aureus*. Initially ZP had a relatively weak effect on the first 2 days but on the third day a significant ($p < 0.05$) decrease occurred.

The cytotoxicity on fibroblasts was evaluated to determine if the peroxides were in anyway selectively toxic against prokaryotic cells or had any compatibility with eukaryotic cells (Figure 5). The results show that the metal peroxides had a negative effect on viability when compared to the control film. Moreover, the viability continues to decrease with time for each metal peroxides-based sample. It appeared that ZP has the least cytotoxicity to human fibroblasts around 80%–70%, followed by CP and then MP. The morphology of the cells reflected this, as the cells became spindle-shaped

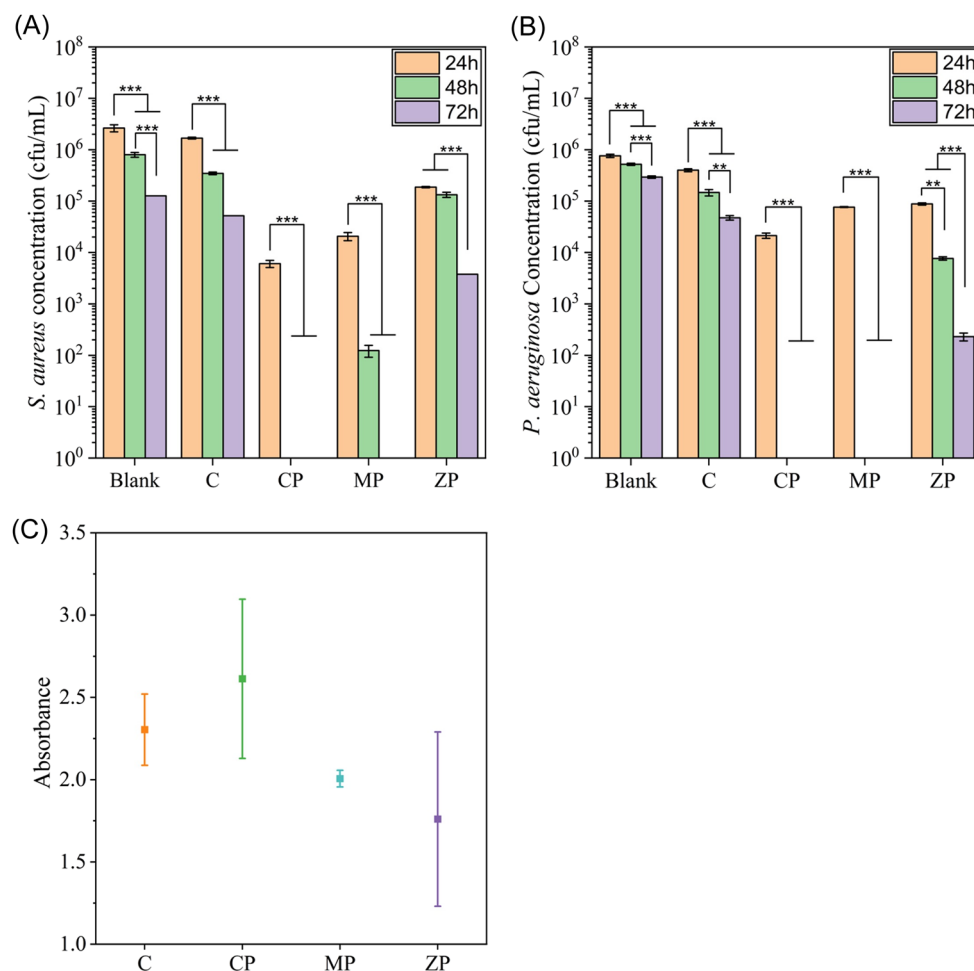


FIGURE 4 Calculated bacterial concentration for (A) *Staphylococcus aureus* and (B) *Pseudomonas aeruginosa* with plate count assays (mean \pm SD; $n = 3$). (C) Biofilm formation with *S. aureus* on control and peroxide-doped PCL (mean \pm SD; $n = 3$). Values indicated by asterisks (*) are statistically different (** $p < 0.01$; *** $p < 0.001$).

and confluent over 3 days only in the control and ZP-treated culture wells, whereas in MP- and CP-treated wells, the cells were more sparse and rounded. There was an absence of cells near all the peroxide-containing sample films that was more pronounced with MP and CP (Figure 5C).

3 | DISCUSSION

A large body of literature focuses on the use of polymers as diffusion barriers to retard peroxide decomposition reaction rates for sustained oxygen release and also as protective barriers to prevent cell and tissue damage, but no prior study has compared the efficacy of decomposition products of inorganic peroxides with regard to their antibacterial performance. This study compared biologically relevant peroxides, CaO₂, ZnO₂, and MgO₂ with different relative solubilities and basicity. The capacity of the polymeric film to absorb and retain water is critical

parameter for assessing its character as a diffusion and protective barrier. PCL has shown potential in wound healing applications due to its very stable structure in aqueous state and the incorporation of peroxides seemed not to affect its morphology or swelling behavior (Figure 1 and Figure S1). The microstructures of the films in this study resembled PCL-inorganic composites with similar loading levels of inorganic particulates processed similarly,³¹ and it was apparent that the inorganic phases were well dispersed.

The extremely low swelling index of peroxide-doped PCL films is attributed to the hydrophobic characteristic of PCL polymers. Given that PCL is a hydrophobic semicrystalline polymer, it is clear that the swelling of the samples was low and that only a small amount of peroxides will degrade after 24 h. Control films had a higher swelling degree than peroxide films, and despite their low porosity, water diffusion through MP and ZP films was more than in CP films (Figure S1) and this parameter would appear a route to further control

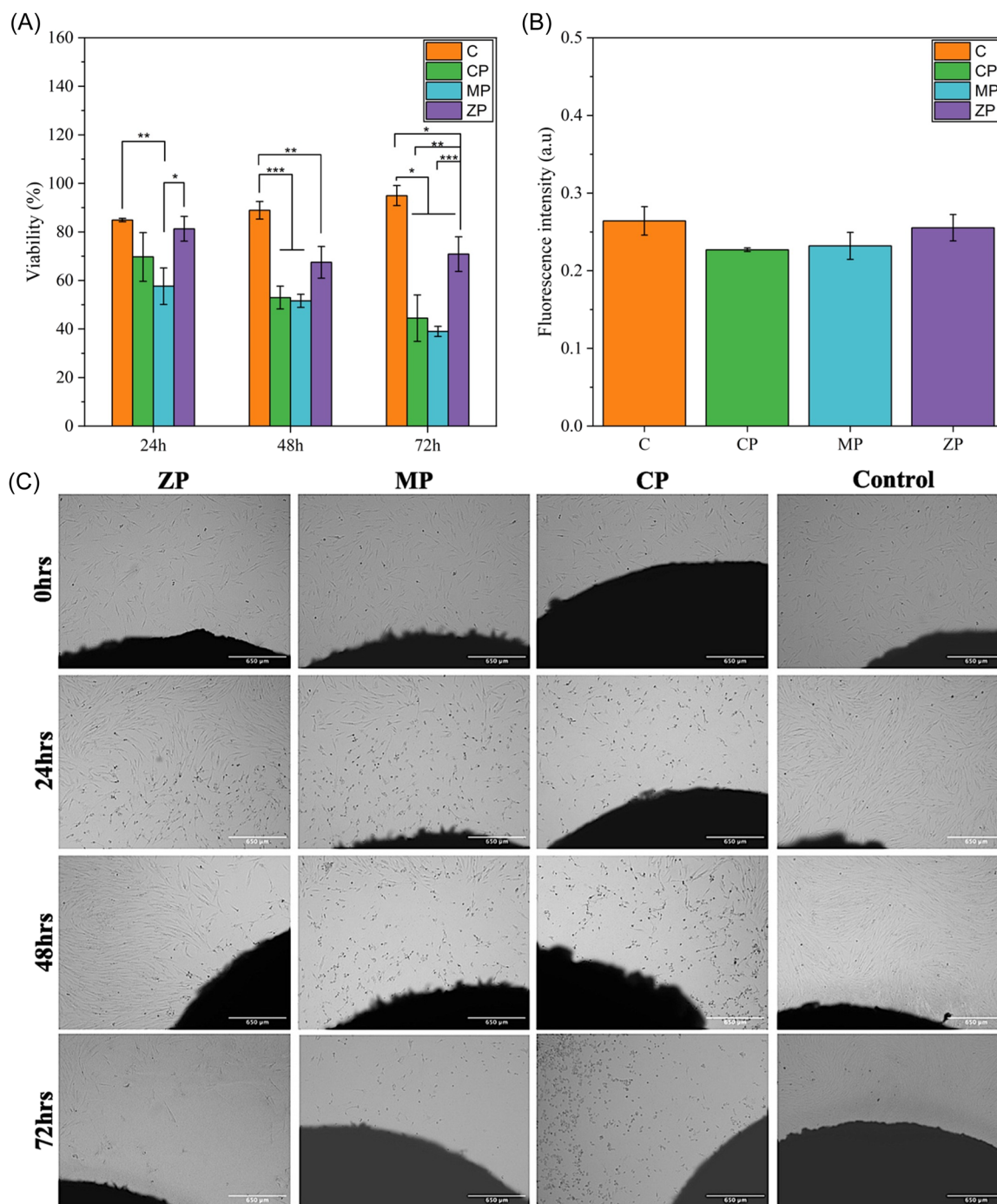


FIGURE 5 (A) Relative percentage (%) of cell viability from human dermal fibroblasts exposed to different peroxide films after 24, 48, and 72 h of incubation (mean \pm SD; $n = 3$). The color-coded columns represent the film composition tested. (B) Fluorescence intensity (mean \pm SD; $n = 3$) of nonquantitative reactive oxygen species measurements after H2DCFDA reagent incubation with HDF cells exposed to each peroxide film after 72 h. (C) Bright-field micrographs ($\times 4$ magnification) captured of different peroxide films in cell culture after 24, 48, and 72 h of incubation. Values indicated by asterisks (*) are statistically different (* $p < 0.05$; ** $p < 0.01$; *** $p < 0.001$).

degradation of reactive fillers. The incorporation of peroxides into PCL film caused a small increase of material stiffness, as determined by increase of Young's modulus and remained higher than skin elasticity, which is estimated at around 140 MPa.³² The values we measured were comparable with ranges reported for

other PCL-inorganic particulate composites which reported film moduli of between 200 and 500 MPa depending on filler loading level.³³

The polymer matrix appeared unreactive toward peroxide since storage at ambient conditions for 18 months resulted in only slight reduction in peroxide

release and one could envisage that with appropriate packaging and protection against humidity, decomposition could be greatly reduced. The antimicrobial activity of the degradation product release of the films was determined by measuring the bacterial concentration with plate count assays (Figure 4). It should be noted that all the samples containing peroxide in our work had activity against *S. aureus* and *P. aeruginosa*, since no decrease in bacterial count was seen for the blank and control films. CP appeared to have a stronger bactericidal effect than MP and ZP. When calcium peroxide reacts in water, they generate Ca^{2+} , O_2 , and H_2O_2 . The antibacterial property of CP is usually associated with the release of H_2O_2 upon degradation,²¹ which is a well-known compound to damage bacterial cells and inhibit their growth.³⁴ In Figure 3C, it can clearly be noticed that H_2O_2 concentration increased with time and was highest for the CP film. Furthermore, the surrounding pH related to the ionic dissociation causing an alkalization of the environment was higher for CP and is also known to play a key role in the antibacterial efficacy.³⁵ The release of Ca^{2+} ions from calcium peroxide has also been reported to elicit an antibacterial effect.³⁶ The generation of ROS which has been found to improve biofilm degradation appeared to be similar between the CP and ZP,³⁷ but the antibacterial effectiveness of ZP was lower than CP and MP. Consequently, ROS appeared to be not a key factor rather the combination of pH and hydrogen peroxide. Another product, metal cations, that is, Ca^{2+} , Zn^{2+} , and Mg^{2+} ions could also contribute to an antibacterial effect. Several studies have investigated the antibacterial effects of magnesium, calcium, and zinc cationic metals. The most studied cation, Zn^{2+} , was found to have a strong antibacterial effect on *Streptococcus mutans* and *Actinomyces naeslundii*³⁸ and to prevent bacterial adhesion by interacting with polysaccharides.³⁹ Ca^{2+} is a critical factor in bacterial physiology; it has been shown to promote bacterial movement, survival reactions, bacterial aggregation, and biofilm formation via cationic bridging and attractive acid-base interactions,⁴⁰ but we are aware of only one study suggesting that Ca^{2+} augments the amount of damage to bacteria during disinfection.⁴¹ To enhance the bactericidal property of Ca^{2+} , mixing Ca^{2+} with Zn^{2+} was found to be an attractive solution as it offered higher antibacterial activity against *S. aureus* than calcium films.⁴² Mg^{2+} ions have been found to have antibacterial properties, but also to independently inhibit biofilm formation in *Bacillus* species by downregulating matrix genes expression.⁴³ Overall, we posit that the initial antibacterial effects

caused by metal peroxides are principally due to the degradation product H_2O_2 and the pH of the environment. Given the contact of dressings with open wounded tissue, biocompatibility should be considered. As expected, the control film did not exhibit obvious cytotoxicity, thus confirming that PCL offers a good cytocompatibility. But peroxide-based films clearly confirmed that the addition of CaO_2 and MgO_2 within the film did significantly affect the cytotoxicity toward mammalian cells after 48 h (30%–40% decrease compared to control), presumably because H_2O_2 release and pH elevation, despite the addition of calcium dihydrogen phosphate monohydrate. ZnO_2 -based films exhibited minimal cytotoxicity with over 70% cell viability at every timepoint. Despite the different ROS release profiles of each film, in vitro tests did not reveal any significant differences of ROS measured between the control film, CP, MP, or Z films cultured with human dermal fibroblasts (HDF) cells after 72 h of exposure. Further studies are needed to evaluate the specific effects of metal peroxide on fibroblast viability and function. Given that bicarbonate buffer system plays a central role in pH buffering in the human body, cytotoxicity associated with pH alkalinity might not be observed in vivo. Strategies to improve biocompatibility will focus on reducing the amount of peroxide in the formulation. The amounts loaded in these studies represented maximal values and it is likely that reducing peroxide loading would reduce toxicity and maintain antibacterial activity. Secondarily the amount of catalyst could then also be reduced which would reduce the amount of oxygen released and more favor hydrogen peroxide formation.

4 | MATERIALS AND METHODS

4.1 | Reagents

Zinc peroxide ZnO_2 (ZP) (481424), magnesium peroxide MgO_2 (MP) (433624), polycaprolactone ($(\text{C}_6\text{H}_{10}\text{O}_2)_n$ (PCL)) (440744), hydrogen peroxide solution H_2O_2 (30%) (1.07298), sodium bicarbonate CHNaO_3 (S5761), Iron (II, III) oxide (637106), chloroform ($\geq 99\%$ $\text{CH}_3\text{Cl}_3\text{C}$), crystal violet (CV) (V5265), acetic acid (33209) were purchased from Sigma-Aldrich. Calcium peroxide CaO_2 (CP) (UN1457) was obtained from FMC Corporation and calcium dihydrogen phosphate monohydrate $\text{Ca}(\text{H}_2\text{PO}_4)$ (AB119788) from ABCR GmbH. Phosphate-buffered saline (PBS) and fluorescein H_2DCFDA (D399) were purchased from Thermo Fisher Scientific (10010031).

TABLE 2 Weight percentage of the components encapsulated in PCL, expressed either as a percentage of the total mass (wt% total), or as a percentage of the amount of polymer used to form the film (wt% polymer).

	Polymer wt%	Peroxide		Fe ₃ O ₄		NaHCO ₃		Ca(H ₂ PO ₄) ₂	
		wt% total	wt% polymer	wt% total	wt% polymer	wt% total	wt% polymer	wt% total	wt% polymer
Sample	66.6	13.7	20.6	13.7	20.6	3.3	0.5	2.7	0.4
Control	77.2	0.0	0.0	15.9	20.6	3.8	0.5	3.1	0.4

4.2 | Composite films

The formulation of the samples was informed by our prior studies into calcium peroxide oxygen release formulations, reducing H₂O₂ release by using iron oxide catalyst, and maintaining a more neutral pH with calcium dihydrogen phosphate monohydrate and sodium bicarbonate addition.^{27,42,44} To form the films, each component was sieved through a 74-μm sieve (ASTM 200 mesh, Gilson company) and added in the ratios shown in Table 2 to 100 mL of 10% w/v PCL solution in chloroform.

Samples with calcium, magnesium, or zinc peroxides were referred to as CP, MP, and ZP films, respectively, and the peroxide-free control sample. The mixture was stirred until homogeneous, poured into a 190 × 100 mm Pyrex crystallizer (PYREX, No. 3140), and left to dry, covered with aluminum foil, at room temperature in a safety hood for 24 h. In this way consistent film thickness was achieved and 6 mm diameter disks were bunched using a standard stationery paper punch. The preparation steps are shown diagrammatically in Figure 6.

4.3 | Composite characterization

The microstructure of the surfaces of the different composites was examined using scanning electron microscopy (15 kV in mixed mode, Hitachi-Hightech TM3030 Plus SEM). The porosity was estimated from SEM images with ImageJ software by adjusting the threshold to highlight the pores. Thermogravimetric analysis (TGA, TA instrument, SDT600) was performed under a nitrogen atmosphere using a heating rate of 4.00°C min⁻¹ up to 1100°C. The swelling index of the samples was measured by drying 6 mm diameter circular specimens of film (*N* = 3). The samples were dried at 60°C for 4 h, then the dried samples were weighed and then immersed in milliQ water for 24 h. Then, the soaked samples were dabbed dry and reweighed. Swelling index was calculated as follows:

$$\text{Swelling Index (\%)} = \frac{W_s - W_d}{W_d}, \quad (1)$$

where W_s is the immersed weight and W_d the initial weight.

4.4 | Release experiments

To analyze the decomposition behavior of the different samples, the conversion of the metal peroxides to O₂ and H₂O₂ was evaluated at 1, 2, 3, 4, 24, and 48 h. Circular films of 6 mm were placed in sealed 1.5 mL microcentrifuge tubes, filled with PBS. Oxygen measurements were made with an oxygen probe (FOSPOR-AL300) connected to the NEOFOX-GT oxygen sensor (Oceaninsight). The probe was calibrated at two points using nitrogen saturated PBS (0% oxygen) and (20.9% oxygen) PBS. A peroxide assay kit (Pierce™ Quantitative Peroxide Assay Kit, Thermo Fisher) was used to measure H₂O₂ concentration. An eight-point standard curve was prepared by diluting 30% H₂O₂ between 0 and 500 μM in PBS to interpret absorbance values. For each sample measurement, 5 μL of the PBS solution in which the sample was inserted into a microplate well, and then 150 μL of reagent solutions were added. The microplate was protected from light by covering it with aluminum foil for 15 min at room temperature. Absorbances were measured at 595 nm with a plate reader (ThermoScientific, Multiskan SkyHigh). Measurements were repeated after 18 months' storage in ambient laboratory conditions. The pH of the PBS was measured using pH probe (Mettler Toledo and a Sartorius sensor) calibrated at 3 points (4, 6, and 10). Finally, the release of all ROS species was evaluated by immersing the 6 mm circular films into 15 ml vials filled with 4 mL of PBS using a chemically reduced form of fluorescein H2DCFDA as an ROS indicator. A 25 μM reagent solution of H2DCFDA was produced by dilution with 99.9% ethanol and used as a probe to measure ROS. Two hundred microliters of the sample solution were added into a black microplate (Corning, 3915) and 5 μL of reagent solution was then added and incubated for 10 min wrapped in aluminum foil at room temperature. ROS release was measured at excitation and emission wavelengths of 488 and 525 nm, respectively. Before each measurement, the solutions were vortexed to be homogeneous.

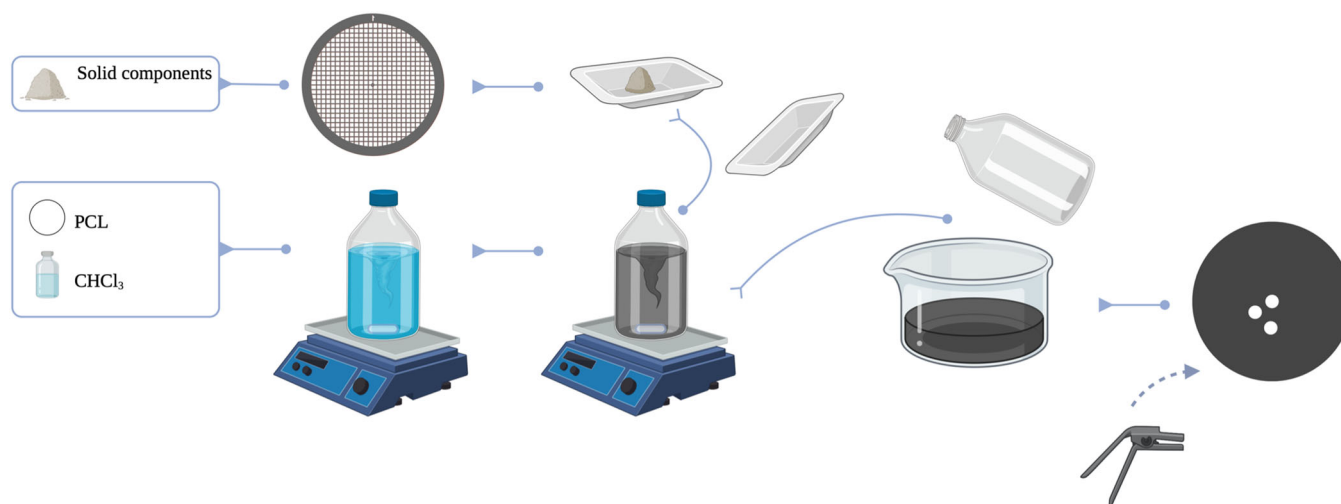


FIGURE 6 Schematic illustration of the composite film processing steps. After sieving the powdered components were added into the polycaprolactone–chloroform solution and mixed thoroughly before being poured into a crystallizer and left to dry. Composite films were generated using a 6 mm diameter circular hole paper-punch for subsequent experimentation. Designed using [Biorender.com](https://www.biorender.com).

4.5 | Mechanical testing

The material was cut into 10 mm × 40 mm samples to assess the mechanical properties for each condition by tensile testing (Instron 3365), a 500 N load cell, at a 5 mm per min-rate, with an active length of 25 mm, up to 10% strain. The material was tested dry. The Young's modulus was calculated from sample dimensions and force/extension data.

4.6 | Cytotoxicity and antioxidant assays

HDF extraction, expansion, and usage received Institutional Review Board (IRB) approval by the MUHC Ethics Research Board (approval #MP-37-2020-5995). HDF cells were used between passages 5 and 8 and subcultured after reaching 75% confluency. HDF cells were grown in DMEM media (Gibco) supplemented with 5% fetal bovine serum (Gibco) and 1% PenStrep (Gibco).

Cytotoxicity was assessed using Alamar Blue (Thermo Fisher). HDF cells were directly plated in a 48-well plate (Thermo Fisher) at a cell density of 3×10^5 in 800 μ L of media. One 6 mm disc of material was added to each well. At 24-, 48-, and 72-h post-seeding, culture medium was aspirated and each well containing cells was rinsed with PBS. In accordance with the manufacturer's instructions (Thermo Fisher), a 10% v/v Alamar blue in fresh medium solution was directly added to each well containing both cells and samples and incubated for 1 h. Following the incubation period, the solution from each well was transferred to a 96-well

black UV F-bottom plate. Top and bottom fluorescent readings were measured at emission/excitation wavelengths of 560/590 nm (Thermo Fisher Varioskan Lux). The resulting readings were averaged for triplicate samples in each condition and divided by the control sample values to obtain relative viability.

Antioxidant tests were conducted using H2DCFDA reagent (Thermo Fisher) in HDF cells following 72 h of exposure to each peroxide film. H2DCFDA was reconstituted in DMSO and diluted to a working concentration of 10 μ M in PBS. Peroxide films were removed from each well and the H2DCFDA solution was incubated for 45 min. The incubated solutions from each well were transferred into a 96-well black UV F-bottom with top and bottom fluorescent readings measured at 485/535 nm emission and excitation wavelengths, respectively.

4.7 | Plate count assays

S. aureus (ATCC 6538) and *P. aeruginosa* (ATCC 15442) (Cedarlane Laboratories). were stored at -80°C until required. To prepare stock cultures, 5 μ L of thawed bacteria was inoculated in 5 mL of LB (Luria-Bertani) broth and incubated at 200 rpm, 37°C for 18 h. The initial concentrations were estimated to be 3×10^{10} and 9×10^9 colony-forming units (CFU) mL^{-1} for *S. aureus* and *P. aeruginosa*, respectively. Then the bacteria strain stock cultures were diluted with nutrient broth (NB 1/500) to achieve the final concentrations of 10^5 CFU mL^{-1} . Nutrient broth was made using ISO 22196:2011 by dissolving 3.0 g of meat extract, 10.0 g of peptone, and

5.0 g of sodium chloride in 1000 mL of distilled or deionized water. The obtained solution was diluted with Milli-Q water to a 500-fold volume and adjusted pH between 6.8 and 7.2. The antibacterial efficacy of the resulting samples was examined through the suspension method. In this respect, CP, MP and ZP, and C films were cut as disks with a size diameter of 6 mm and suspended into the 5 mL diluted bacteria species. The samples were incubated at 37°C, 200 rpm and at varied incubation times, 24, 48, and 72 h. Control samples were considered under similar conditions, excluding samples with an antibacterial agent. At the end of the incubation period, 100 µL of aliquots were taken to prepare four serial dilutions with a dilution factor of ten in the saline buffer. Then, the viable bacterial counts were enumerated by spreading 100 µL of diluted aliquots on to the agar Petri dishes incubated overnight at 37°C. All experiments were repeated in triplicate. Viable bacteria concentration was calculated considering all dilutions made according to the following equation:

$$\text{concentration (cfu.mL}^{-1}\text{)} = \frac{n \times d}{V}, \quad (2)$$

where n is the number of colonies (average of three replicates), d the dilution factor, and V the volume of culture plate in mL ($V = 100 \mu\text{L}$). A solution without samples was used as a basis for comparison referred to as the blank.

4.8 | Biofilm assays

CV solution 1% and acetic acid were diluted to 0.1% and to 33%, respectively, with milli-Q water. *S. aureus* and *P. aeruginosa* bacterial strains were also used to conduct a biofilm formation assay. A bacterial stock solution was again prepared by inoculating 10 µL of dehydrated bacteria in 5 mL LB broth and incubated at 200 rpm, 37°C for 17–18 h. The stock solution was diluted with LB broth to obtain a 10^5 CFU mL^{-1} bacterial solution. One milliliter of this bacterial solution was incubated with triplicate samples of each condition (C, CP, MP, ZP in triplicates) in a 48-well plate, with shaking at 37°C, for 72 h. Control material to account for the stain absorption was also added to LB in triplicate.

The biofilm formation was then assessed by CV staining: CV stains the biofilm and is released in acetic acid, which allows the quantification of biofilm by an absorbance measurement. The excess bacterial solution in the wells was discarded by careful pipetting, in

order not to disturb the biofilm at the surface of the samples. The samples were carefully transferred to a clean well before drying for 30 min at 50°C in an incubator, to dry the biofilm. One hundred and fifty microliters of 0.1% CV stain was added to each well and left to incubate for 15 min at room temperature. The wells were then rinsed well with 500 µL milli-Q water at a time until the rinsing solution is clear, to remove the excess CV not staining for biofilm. The samples were left to dry at room temperature before adding 350 µL of 33% acetic acid and incubating for another 15 min, with occasional gentle manual shaking. One hundred microliters triplicates were pipetted from each well into a 96-well plate, along with 100 µL 33% acetic acid for background. The absorbance at 570 nm was read with a microplate reader (Tecan, Infinite F500). The absorbance of the control sample without bacteria and the background were subtracted from the absorbance of the various conditions before analysis.

4.9 | Statistical analysis

All results were expressed as mean \pm standard deviation ($N = 3$) and were normalized by molar mass. Statistical significance was assessed by one-way ANOVA followed by a Tukey post-hoc test. p Values < 0.05 were considered statistically significant.

5 | CONCLUSION

In this study, we successfully developed peroxide-doped polymeric films with promising potential for wound healing and antibacterial applications. The incorporation of calcium, magnesium, or zinc peroxide into a biocompatible polymeric film resulted in efficient prevention of the growth of both Gram-positive and Gram-negative bacteria. The films also demonstrated sustained release of reactive oxygen species and oxygen, contributing to their prolonged antibacterial activity. In vitro experiments utilizing human dermal fibroblasts showed a moderate degree of biocompatibility toward fibroblasts. The unique combination of antibacterial efficacy and mammalian cell biocompatibility makes these films a promising advancement for various medical applications, including wound dressings, coatings, and other healthcare products. Further studies involving in vivo evaluations are warranted to fully explore the translational potential of peroxide-based materials.

AUTHOR CONTRIBUTIONS

Conceptualization: Dario Job, Jake Barralet, and Geraldine Merle. **Methodology:** Dario Job, Justin Matta, Cat-Thy Dang, Bentolhoda Helli, and Joshua Vorstenbosch. **Validation:** Dario Job, Justin Matta, Cat-Thy Dang, and Yara Raphael. **Formal analysis:** Dario Job, Justin Matta, and Cat-Thy Dang. **Resources:** Jake Barralet, Geraldine Merle and Joshua Vorstenbosch. **Data curation:** Dario Job, Justin Matta, and Cat-Thy Dang. **Writing—original draft preparation:** Dario Job. **Writing—review and editing:** Jake Barralet and Geraldine Merle. **Supervision:** Geraldine Merle. **Funding acquisition:** Geraldine Merle and Jake Barralet. All authors have read and agreed to the published version of the manuscript.

ACKNOWLEDGMENTS

We acknowledge the use of BioRender in the production of Figure 6. This research was funded by NSERC discovery grants (Geraldine Merle and Jake Barralet) and FRQS chercheur boursier J1 (Geraldine Merle).

CONFLICT OF INTEREST STATEMENT

The authors declare no conflict of interest.

DATA AVAILABILITY STATEMENT

Data can be made available upon request.

ETHICS STATEMENT

HDF extraction, expansion, and usage received Institutional Review Board (IRB) approval by the MUHC Ethics Research Board (approval #MP-37-2020-5995).

ORCID

Geraldine Merle  <http://orcid.org/0000-0001-8044-985X>

REFERENCES

- Hutchings MI, Truman AW, Wilkinson B. Antibiotics: past, present and future. *Curr Opin Microbiol*. 2019;51:72-80.
- Murray C, Ikuta KS, Sharara F, et al. Global burden of bacterial antimicrobial resistance in 2019: a systematic analysis. *Lancet*. 2022;399(10325):629-655.
- Windels EM, Michiels JE, Van den Bergh B, Fauvart M, Michiels J. Antibiotics: combatting tolerance to stop resistance. *mBio*. 2019;10(5):e02095-19.
- Peters BM, Shirliff ME, Jabra-Rizk MA. Antimicrobial peptides: primeval molecules or future drugs? *PLoS Pathog*. 2010;6(10):e1001067.
- Shai Y. Mode of action of membrane active antimicrobial peptides. *Pept Sci*. 2002;66(4):236-248.
- Zhang L, Rozek A, Hancock REW. Interaction of cationic antimicrobial peptides with model membranes. *J Biol Chem*. 2001;276(38):35714-35722.
- Andersson DI, Hughes D, Kubicek-Sutherland JZ. Mechanisms and consequences of bacterial resistance to antimicrobial peptides. *Drug Resist Updates*. 2016;26:43-57.
- Bechinger B, Gorr SU. Antimicrobial peptides: mechanisms of action and resistance. *J Dent Res*. 2017;96(3):254-260.
- Sherman Won. The abortive treatment of wound infection: Carrel's method-Dakin's solution. *JAMA*. 1917;LXIX(3):185-192.
- Reid MR, Altemeier WA. Peroxide ointments. *Ann Surg*. 1943;118(4):741-750.
- Ottesen TD, Qudsi RA, Kahanu AK, et al. The continued utility and viability of Dakin's solution in both high- and low-resource settings. *Archiv Bone Jt Surg*. 2020;8(2):198-203.
- Duarte B, Cabete J, Formiga A, Neves J. Dakin's solution: is there a place for it in the 21st century? *Int Wound J*. 2017;14(6):918-920.
- Meleney FL. Present role of zinc peroxide in treatment of surgical infections. *JAMA*. 1952;149(16):1450-1453.
- Kligman AM, Leyden JJ, Stewart R. New uses for benzoyl peroxide: a broad-spectrum antimicrobial agent. *Int J Dermatol*. 1977;16(5):413-417.
- Cui H, Liu M, Yu W, et al. Copper peroxide-loaded gelatin sponges for wound dressings with antimicrobial and accelerating healing properties. *ACS Appl Mater Interfaces*. 2021;13(23):26800-26807.
- Lin L-S, Huang T, Song J, et al. Synthesis of copper peroxide nanodots for H₂O₂ self-supplying chemodynamic therapy. *J Am Chem Soc*. 2019;141(25):9937-9945.
- Wang H, Zhao Y, Li T, Chen Z, Wang Y, Qin C. Properties of calcium peroxide for release of hydrogen peroxide and oxygen: a kinetics study. *Chem Eng J*. 2016;303:450-457.
- Shen S, Mamat M, Zhang S, et al. Synthesis of CaO₂ nanocrystals and their spherical aggregates with uniform sizes for use as a biodegradable bacteriostatic agent. *Small*. 2019;15(36):1902118.
- Thi PL, Lee Y, Tran DL, Hoang Thi TT, Park KM, Park KD. Calcium peroxide-mediated in situ formation of multi-functional hydrogels with enhanced mesenchymal stem cell behaviors and antibacterial properties. *J Mater Chem B*. 2020;8(48):11033-11043.
- Azine Z, Moeini M, Solouk A, Akbari S. Polyurethane-calcium peroxide composite nanofibrous scaffolds with controlled oxygen release for tissue engineering applications. *Nano*. 2023;18(2):2350012.
- Wu X, Han X, Guo Y, et al. Application prospect of calcium peroxide nanoparticles in biomedical field. *Rev Adv Mater Sci*. 2023;62(1):20220308.
- Zhang M, Song R, Liu Y, et al. Calcium-overload-mediated tumor therapy by calcium peroxide nanoparticles. *Chem*. 2019;5(8):2171-2182.
- Steg H, Buizer AT, Woudstra W, et al. Control of oxygen release from peroxides using polymers. *J Mater Sci Mater Med*. 2015;26(7):207.
- Pedraza E, Coronel MM, Fraker CA, Ricordi C, Stabler CL. Preventing hypoxia-induced cell death in beta cells and islets via hydrolytically activated, oxygen-generating biomaterials. *Proc Natl Acad Sci*. 2012;109(11):4245-4250.
- Fu Y, Kao WJ. Drug release kinetics and transport mechanisms of non-degradable and degradable polymeric delivery systems. *Expert Opin Drug Deliv*. 2010;7(4):429-444.
- Rambhia KJ, Ma PX. Controlled drug release for tissue engineering. *J Controlled Release*. 2015;219:119-128.

27. Rastinfard A, Dalisson B, Barralet J. Aqueous decomposition behavior of solid peroxides: effect of pH and buffer composition on oxygen and hydrogen peroxide formation. *Acta Biomater.* 2022;145:390-402.
28. National Center for Biotechnology Information. PubChem Compound Summary for CID 516892, Sodium Bicarbonate. Accessed January 13, 2024. <https://pubchem.ncbi.nlm.nih.gov/compound/Sodium-Bicarbonate>
29. Ropp RC. Chapter 3—Group 16 (O, S, Se, Te) alkaline earth compounds. In: Ropp RC, ed. *Encyclopedia of the Alkaline Earth Compounds*. Elsevier; 2013:105-197.
30. Hu H, Yu L, Qian X, Chen Y, Chen B, Li Y. Chemoreactive nanotherapeutics by metal peroxide based nanomedicine. *Adv Sci (Weinh)*. 2020;8(1):2000494.
31. Holešová S, Čech Barabaszová K, Hundáková M, et al. Development of novel thin polycaprolactone (PCL)/clay nanocomposite films with antimicrobial activity promoted by the study of mechanical, thermal, and surface properties. *Polymers*. 2021;13(18):3193.
32. Joodaki H, Panzer MB. Skin mechanical properties and modeling: a review. *Proc Inst Mech Eng Part H*. 2018;232(4):323-343.
33. Wei J, Heo SJ, Kim DH, Kim SE, Hyun YT, Shin JW. Comparison of physical, chemical and cellular responses to nano- and micro-sized calcium silicate/poly(ε-caprolactone) bioactive composites. *J R Soc Interface*. 2008;5(23):617-630.
34. Singh A, Dubey AK. Various biomaterials and techniques for improving antibacterial response. *ACS Appl Bio Mater*. 2018;1(1):3-20.
35. Siqueira Jr. JF, de Uzeda M. Influence of different vehicles on the antibacterial effects of calcium hydroxide. *J Endod*. 1998;24(10):663-665.
36. Christian DG, Miller DP. Effect of a calcium peroxide seed coating on the establishment and yield of winter wheat sown by direct drilling in the presence of straw residues. *J Sci Food Agric*. 1984;35(6):606-608.
37. Hata Y, Bouda Y, Hiruma S, Miyazaki H, Nakamura S. Biofilm degradation by seashell-derived calcium hydroxide and hydrogen peroxide. *Nanomaterials*. 2022;12(20):3681.
38. Nishida E, Miyaji H, Shitomi K, Sugaya T, Akasaka T. Evaluation of antibacterial and cytocompatible properties of multiple-ion releasing zinc-fluoride glass nanoparticles. *Dent Mater J*. 2021;40(1):157-164.
39. Steiger EL, Mueller JR, Braissant O, Waltimo T, Astasov-Frauenhoffer M. Effect of divalent ions on cariogenic biofilm formation. *BMC Microbiol*. 2020;20:287.
40. Körstgens V, Flemming HC, Wingender J, Borchard W. Influence of calcium ions on the mechanical properties of a model biofilm of mucoid *Pseudomonas aeruginosa*. *Wat Sci Technol*. 2001;43(6):49-57.
41. Xu Z, Liu X, Feng C, et al. Disinfection properties of the tea polyphenol epigallocatechin gallate in the presence of calcium ions. *Aqua Water Infrastruct Ecosyst Soc*. 2021;70(5):731-740.
42. Ouhaddi Y, Dalisson B, Rastinfard A, et al. Necrosis reduction efficacy of subdermal biomaterial mediated oxygen delivery in ischemic skin flaps. *Biomater Adv*. 2023;153:213519.
43. Oknin H, Steinberg D, Shemesh M. Magnesium ions mitigate biofilm formation of *Bacillus* species via downregulation of matrix genes expression. *Front Microbiol*. 2015;6:907.
44. Product Sheet: alamarBlue Cell Viability Reagent. Accessed January 13, 2024. <https://www.thermofisher.com/document-connect/document-connect.html?url=https://assets.thermofisher.com/TFS-Assets%2FSLG%2Fmanuals%2FAlamarBluePIS.pdf>

SUPPORTING INFORMATION

Additional supporting information can be found online in the Supporting Information section at the end of this article.

How to cite this article: Job D, Matta J, Dang C-T, et al. Comparison of antimicrobial properties of inorganic peroxide polymer composites. *MedComm – Biomater Appl*. 2024;3:e75. doi:10.1002/mba2.75